UJMR, Vol. 10 No. 1, June, 2025, pp. 230 - 243 *E-ISSN: 2814 – 1822; P-ISSN: 2616 – 0668*

https://doi.org/10.47430/ujmr/25101.023

Received: 14/ 01/2025 **Accepted:** 12/06/2025

Green Synthesis, Optimization, and Characterization of Copper Nanoparticles Using a Combined Extract of Selected Plant Seeds

Aliyu Shehu*, Okunola Oluwole Joshua and Uduma A. Uduma
Department of Chemistry, Federal University Dutsin-ma, Katsina state, Nigeria.
Correspondence: aslyyaradua@gmail.com

Abstract

This work investigates a verde method involving synthesizing, optimizing, and characterizing copper nanoparticles (CuNPs) developed from black seed, neem seed, and baobab seed extracts. The optimal synthesis conditions were investigated by means of a Taguchi method. UV-Vis spectroscopy was used to confirm the formation of CuNPs, which exhibited an SPR peak of 590.10 nm (Fig. 1), indicating the nanoparticles' presence. Characteristic peaks at 566.65, 984.04, 1088.47, 1632.62, 2117.12, and 3265.16 cm^{-1} were observed, attributing to Cu-O and Cu-OH and Cu-O-C bonds, as well as hydroxyl and carbon dioxide functional groups, indicating an effective capping and stabilization of the nanoparticles by plant phytochemicals (FTIR analysis). The crystalline nature of CuNPs has been confirmed using X-ray diffraction analysis, which gave diffraction peaks at 22.43°, 47.07°, 67.12°, and 87.33°. The particle size was found to be 25.51 nm. The particles exhibited a mostly spherical shape with some degeneracy when analyzed by scanning electron microscopy (SEM), and the elemental composition (EDX) characterized a copper content of 45.3% and additional plant-derived stabilizing agents, such as carbon, oxygen, and trace elements. Besides, the antimicrobial assay showed potent inhibitory effects on multiple pathogenic microbes. The CuNPs showed significant antibacterial activity, exhibiting maximum inhibition zones against Acinetobacter baumannii (17 mm) and Escherichia coli (19 mm). These results emphasize the potential of biogenically synthesized CuNPs as potential antimicrobial agents and sustainable alternatives for biomedical and pharmaceutical applications.

Keywords: Acinetobacter baumannii, antibacterial, copper nanoparticles (CuNPs), Escherichia Coli, green synthesis, nanoparticles.

INTRODUCTION

Nanotechnology has made great strides, resulting in the development of high-tech materials that exhibit special physicochemical properties. Metal nanoparticle biosynthesis has gained interest in recent years because it is relatively eco-friendly and cost-effective compared to traditional chemical methods (Ajitha *et al.*, 2015). Plant extracts, for their content of bio-active compounds, including polyphenols, flavonoids, terpenoids, and alkaloids, are widely used as reducing and stabilizing agents in nanoparticle synthesis (Gurunathan *et al.*, 2014). Apart from reducing the metal ions, these biomolecules stabilize and cap the nanoparticles, which ensures their stability. When reduced to nanoscale, metals can exhibit properties far superior to their bulk counterparts and therefore, have numerous applications in areas ranging from antimicrobial to catalysis to optics. Traditional methods of synthesizing nanoparticles such as chemical reduction and physical vapor deposition often involve toxic reagents and consume lots of energy. These constraints have prompted interest in more environmentally friendly alternatives in which plant extracts can be natural reducing agents (Gurunathan *et al.*, 2014). Several studies have proved the synthetical ability of the CuNPs through plants in which plant-derived biomolecules were found involved in the process of reduction and stabilization. For instance, Ajitha et al. (2015) got CuNPs with plant extracts and emphasized that plant metabolites could favor the formation of nanoparticles. Analytical characterization of metal nanoparticles due to their unique physicochemical properties is critical.

The UV-Vis spectroscopy is generally used to confirm nanoparticle synthesis via surface plasmon resonance (SPR) peak. In FTIR spectroscopy, information about the functional groups responsible for nanoparticle stabilization can be obtained by detecting the interactions between biomolecules and metallic ions.

Crystalline structure and phase composition were characterized by X-ray diffraction (XRD), and scanning-electron microscopy (SEM) and

energy-dispersive X-ray spectroscopy (EDX) were used to analyze nanoparticle morphology and elemental composition. SEM captures high-resolution images that show nanoparticle size, shape, and surface texture, while EDX identifies elemental constituents. A study by Gurunathan et al. (2014) confirmed SEM and EDX to show specific morphological characteristics with different elemental compositions which can be attributed to metal nanoparticles. Metal nanoparticles have many applications, but their antimicrobial properties are most promising in the fight against antibiotic resistance. Copper nanoparticles have garnered significant research interest due to their potent antimicrobial activity, which has been attributed to three properties: their potential to disrupt microbial membranes, denature proteins, and induce oxidative stress, ultimately resulting in cell death. They are efficacious against microbes of various genera, with studies documenting considerable antibacterial activity against Gram-positive and Gram-negative bacteria. Research by Kenneth *et al*. (2023) showed that CuNPs synthesized by Justicia schimperiana leaf extract displayed potent antibacterial activity against *Pseudomonas aeruginosa* and *Bacillus subtilis*.

To evaluate their antimicrobial efficacy, the current study was designed to biosynthesize the CuNPs using extracts of three medicinal plant seeds: black seed, neem seed, and baobab seed. Nanoparticles from biogenic (living organisms) sources have been shown to associate with bacterial membranes, resulting in subsequent structural disruption leading to bacterial cell death. This study aims to optimize, synthesize, characterize, and investigate the antimicrobial activity of CuNPs as alternative antimicrobial agents against Gram-positive and Gram-negative bacteria and fungal pathogens.

MATERIALS AND METHODS

Materials

Neem seed, Black seed, Baobab seed, Sodium hydroxide (99%), Copper sulphate (99%), Ethanol (99%), Mueller hinton agar, glass wares, teplon containers, filter papers, crucibles, Rotary evaporator (Rotavapor R-210), Incubator (Thermo scientific incubator), pH meter (Mettler-Tolado pH meter), UV-Vis spectrometer (Shimadzu UV-1800), FTIR spectrometer (Shimadzu XRD-600), SEM/EDX (Hitachi SU-70 SEM/EDX).

Methods

Sample Collection and Identification

Fresh seeds of the neem (*Azadirachta indica*), and baobab (*Adansonia digitata*) were obtained from Ajiwa village in Batagarawa local government Katsina farmland. Black seed (Nigella sativa) Seeds were obtained from Sabon Gari Market, Kano state. The samples were identified at the Biology Department of Umaru Musa Yaradua University Katsina.

Sample Preparation

The seeds were cleaned to eliminate dirt, debris, and other foreign materials. They were then washed extensively with distilled water and air-dried in a shaded and ventilated environment at ambient temperature (30°C) for 10 days. The seeds were dried and then re-milled on a mechanical mill, followed by a sieving process to create a uniform particle size. The powdered samples were added to airtight containers (Ali *et al.*, 2020). A modified method by Zhang *et al*. (2018) for preparing crude extracts was followed. About 50g of each powdered plant seed sample was weighed and mixed with 500 mL of Ethanol in conical flasks. The flasks were capped with aluminum foil and macerated at room temperature for 48 hours. At the end of the maceration period, the extracts were filtered through Whatman No. 1 filter paper to separate the liquid phase. Filtrates were then concentrated by a rotary evaporator and stored until analysis.

Optimization of the Biosynthesis of Copper Nanoparticles (Using Taguchi Method)

An enhanced protocol for copper nanoparticle synthesis was developed based on the method described by Singh and Bhardwaj (2022). The best synthesis conditions were established using the Taguchi method, which involved choosing a suitable orthogonal array method to test the main factors, including the temperature, pH, plant extract concentration, stirring speed, and reaction time. Nanoparticles over synthesis were studied considering four distinct levels well known to researchers for each factor. UV-Vis measured absorbance for each standard, and the UV-Vis measurement was chosen as the optimal synthesis condition. These values were then used to biosynthesize the nanoparticles.

Biosynthesis of Copper Nanoparticles Using Optimal Condition

The procedure for synthesizing copper nanoparticles from the combined crude extract of neem seed, black seed, and baobab seed was adopted with slight modification from the method by Kaur and Dhillon (2023).

About 0.2497g of $CuSO_4$. 1mM $CuSO_4$ was made by dissolving 0.4g of $CuSO_4 \cdot 5H_2O$ in 1000mL distilled water. About 25mL of the combined plants' crude extract and 90mL of prepared 1mM $CuSO_4$ were added into a conical flask.

Then, adjust the pH of the solution with NaOH solution to pH 11, and then place the mixed solution on the magnetic stirrer and stir for 30 minutes at a constant temperature of 80℃ until color change (from yellow-green to reddish brown) occurred which is the sign of the formation of copper nanoparticles, the solution is scanned using a UV-Vis spectrometer at a wavelength range of 300 to 700nm, and the appearance of the absorption peak at a wavelength of 550-600nm is indicating the formation of the nanoparticles. The particles were separated by centrifuging the solution at 4000 rpm for 20 minutes. The precipitated nanoparticles were washed with distilled water to remove unreacted components and then dried at room temperature using an incubator to obtain nanoparticle powder. The resulting dried CuNPs were preserved in a sealed plastic container for further analysis.

Characterization of Biosynthesized Nanoparticles

UV-Vis Analysis

The synthesized nanoparticles were then diluted with distilled water (1:10) and placed into a clean quartz cuvette for spectral analysis. The absorption spectra were plotted in the wavelength range from 200 to 700 nm. Nanoparticle formation was monitored by examining the intensity and location of the absorption peak and estimating the particle size. The distinct peak at the approximate wavelength confirmed the successful synthesis of the nanoparticles (Saharan *et al.*, 2019).

FTIR Analysis

The biosynthesized dried nanoparticle powder was mixed in KBr and scanned at a spectral range of 4000–400 cm^{-1} in Fourier-transform infrared (FTIR) spectroscopy. Characteristic peaks associated with functional groups such as O–H, C=O, and N–H were further analyzed from the obtained spectra. These peaks revealed the biomolecules responsible for capping and stabilizing the nanoparticles, such as proteins and secondary metabolites from the plant extract (Zhao and Zhang, 2020).

SEM/ EDX Analysis

Bacterial cultures were spread evenly onto the surface of each agar plate with a sterile swab and allowed to dry for 3–5 minutes to remove excess moisture. The prepared nanoparticle solutions were added at various concentrations to each well and incubated at 37°C for 24 h. The antimicrobial efficacy of nanoparticles was evaluated by measuring the diameter of

The nanoparticle solution was prepared on a clean SEM stub by drop-casting to form a thin film and dried at ambient conditions. A thin gold coat was deposited on the surface to avoid surface charging during imaging. After that, the nanoparticle sample was mounted in a SEM chamber with the yawning parameters adjusted at the refined fields of 5–20 kV. Images were taken to analyze the morphology (size, shape, and distribution) of interest in the region-color focused to varying magnification. This was followed by an energy-dispersive X-ray (EDX) spectroscopy for the analysis of the elemental composition of the nanoparticles. The characteristic peaks of the associated elements in EDX spectra indicated the metallic nature of the prepared nanoparticles, as reported elsewhere (Dinesh *et al.*, 2021).

XRD Analysis

The powdered nanoparticles were ground well for uniformity in analysis, and the sample was evenly spread on the glass slide. The sample was mounted on an XRD sample holder, and the scanning angle (2θ) was adjusted to range from 10° to 80°, a common range used for metal nanoparticles. The pattern was recorded at a scanning rate of 0.02°/s and the diffraction peaks were used to analyze the crystalline structure of the nanoparticles, comparing them with standard reference patterns of the JCPDS. The peak positions confirmed the various nanoparticle phases (e.g., Ag, Cu, or Zn), and the broadness of the peak was used to calculate crystallite size via the Scherrer equation (Patil *et al.*, 2019).

Antimicrobial Analysis

The antimicrobial activity of the biosynthesized nanoparticles was assessed by performing the disc diffusion method in accordance with the National Committee for Clinical Laboratory Standards guidelines (NCCLS). The stock solutions of the nanoparticles were prepared in the concentrations of 500 ppm, 250 ppm, 125 ppm, 62.5 ppm, and 32.5 ppm by serial dilution. The antimicrobial activity was evaluated using Mueller-Hinton Agar plates. Prior to the inoculation, 6 mm wells were punctured aseptically into the agar medium with a sterile borer. The test bacterial strains were standardized to a 0.5 McFarland standard solution for matching concentrations of bacteria.

inhibition zones, expressed in millimeters, using a metric ruler after incubation (Vivekanandhan and Saravanan, 2021).

MIC Test

The dilution method was used to determine the minimum inhibitory concentration (MIC). Each nanoparticle fraction that showed antimicrobial activity was emulsified at the lowest concentration (which displayed antimicrobial properties) in serial dilutions in test tubes containing Mueller-Hinton Broth. The tubes were then inoculated with equal volumes of bacterial or fungal inoculum and the nanoparticle fractions. A single colony of each isolate was inoculated into 5 mL of sterile Cadebro broths (Oxoid), incubated at 37°C for 24 h for bacteria and at 25°C for 48 h for fungi. For accuracy, three control tubes were kept for each strain: a media, organism, and nanoparticle control. The MIC was determined as the minimum concentration (largest dilution), showing no visible microbial growth (no turbidity) compared to control tubes (Saharan *et al.*, 2019).

MBC Test

For the determination of minimum bactericidal concentrations (MBC), an aliquot from those MIC test tubes showing no obvious growth was subcultured on freshly prepared nutrient agar plates. The plates were then incubated again at 37°C for 24 hours. The maximum dilution at which no bacterial colonies were seen on the agar surface was defined as the maximum bacterial count (MBC). The same was done for fungi, but the plates were incubated at 25°C for 42 h. MFC was defined as the highest dilution at which no fungal colonies were observed (Jain and Singh, 2021).

RESULTS AND DISCUSSION

Results

Optimization of the Biosynthesis of Copper Nanoparticles Results

Table 1. Optimization of Copper Nano Particle Synthesis

Std	Run	Block	A	B	C	D	E	Absorbance
3	1	Block 1	1	3	3	3	3	0.45
14	2	Block 1	4	2	3	1	4	0.30
15	3	Block 1	4	3	2	4	1	0.60
9	4	Block 1	3	1	3	4	2	0.15
11	5	Block 1	3	3	1	2	4	0.60
10	6	Block 1	3	2	4	3	1	0.15
1	7	Block 1	1	1	1	1	1	0.30
4	8	Block 1	1	4	4	4	4	0.45
16	9	Block 1	4	4	1	3	2	0.45
13	10	Block 1	4	1	4	2	3	0.60
12	11	Block 1	3	4	2	1	3	0.15
8	12	Block 1	2	4	3	2	1	0.30
6	13	Block 1	2	2	1	4	3	0.45
2	14	Block 1	1	2	2	2	2	0.15
5	15	Block 1	2	1	2	3	4	0.60
7	16	Block 1	2	3	4	1	2	0.30

Characterization of Biosynthesized Nanoparticles

CuNPs Uv-Vis Result

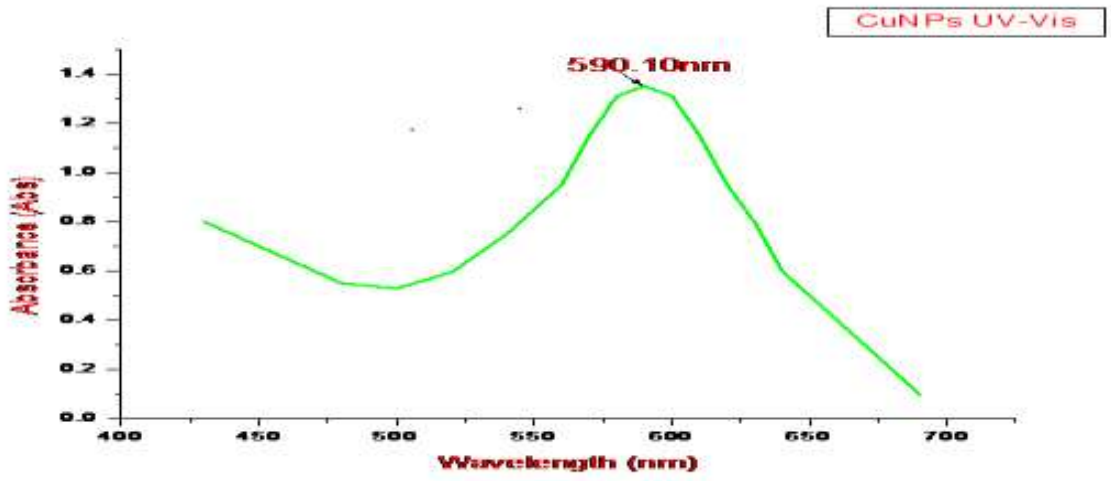

Figure 1. UV-Vis Spectra of CuNPs

CuNPs FTIR Result

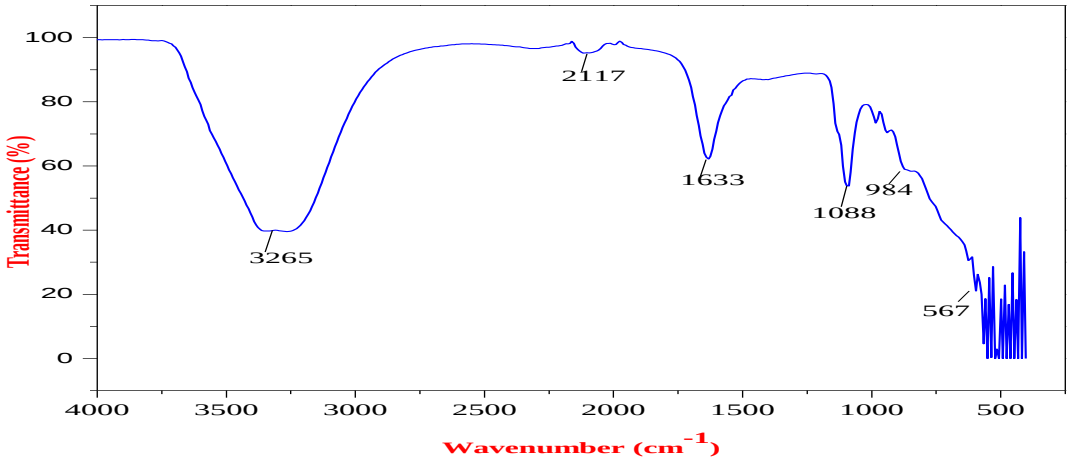

Figure 2. CuNPs FTIR Spectra

Table 2. CuNPs FTIR

S/N	Wavelength (cm^{-1})	Intensity	Functional groups
1	566.65894	4.55046	Cu-O
2	984.04455	73.3672	Cu-OH
3	1088.4724	53.7650	Cu-O
4	1632.6243	62.1923	HOH
5	2117.1234	95.1993	CO_2
6	3265.1684	39.5184	OH

CuNPs SEM/EDX Result

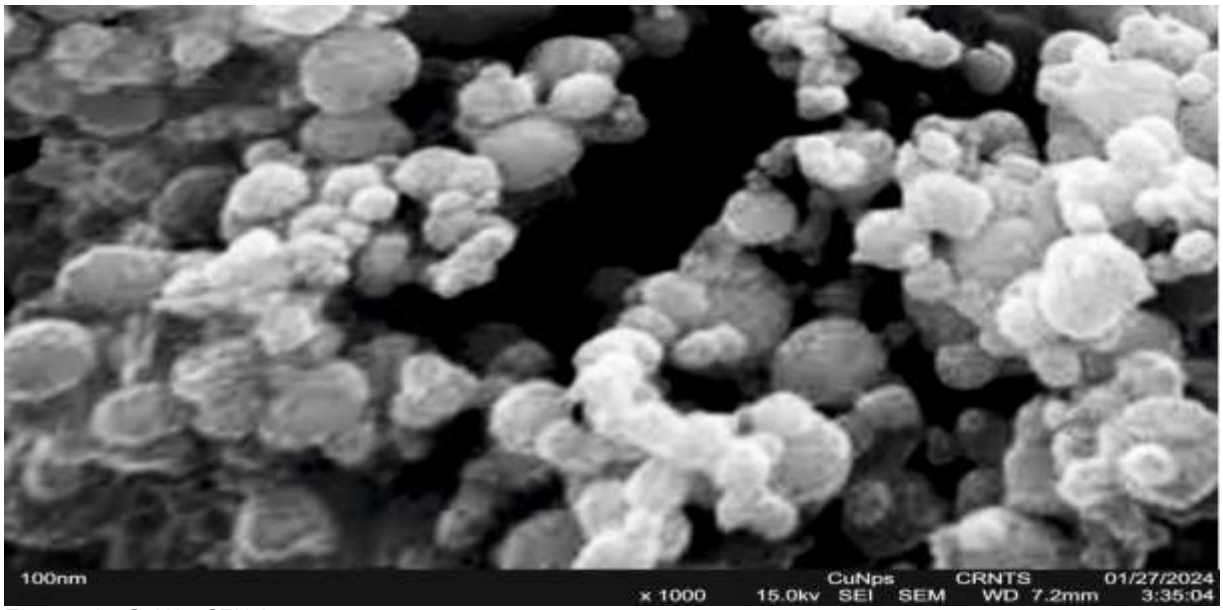

Figure 3. CuNPs SEM Image

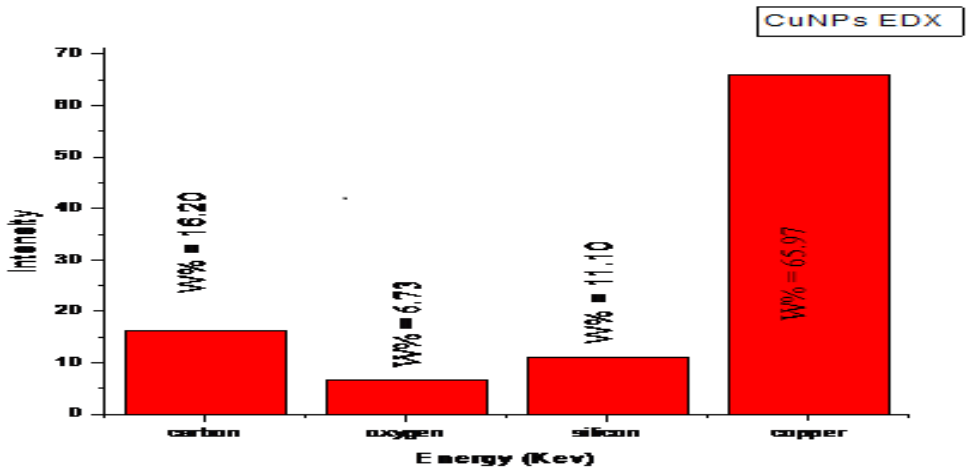

Figure 4. CuNPs EDX

CuNPs XRD Result

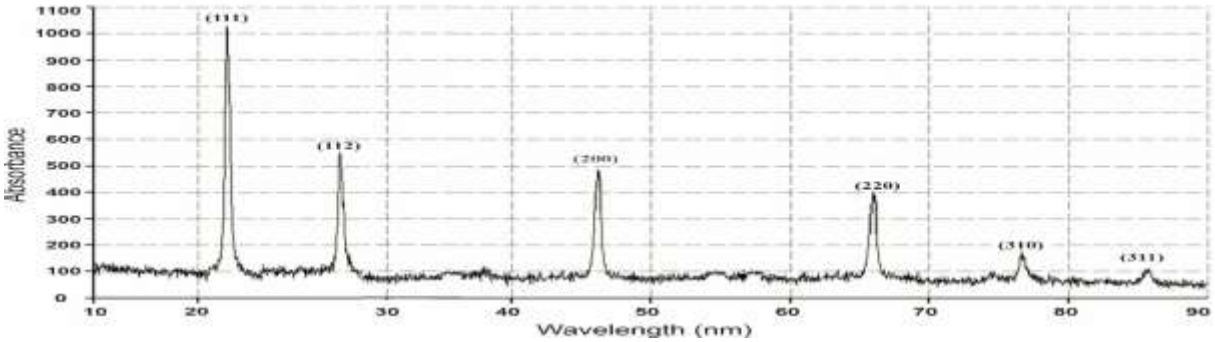

Figure 5. CuNPs XRD Spectra.

Table 3. Determination of the average size of the CuNPs

Position (nm)	Height (ABS)	FWHM(nm)	d-Spacing (A)	Particle Size (nm)
22.43	1047.34	0.644	0.149	29.5
27.96	561.29	0.689	0.148	29.4
47.02	495.38	0.694	0.144	27.3
67.12	410.11	0.798	0.131	26.4
78.01	278.89	0.877	0.126	22.4
87.33	121.43	0.939	0.121	18.5

NOTE: The average particle size = 25.51nm

Antimicrobial Analysis Result

Table 4. Antibacterial Activity of CuNPs (Gram Negative and Gram Positive Bacteria species)

S/N	Concentration (ppm)	*A. baumannii* (mm)	*E. coli* (mm)	*K. pneumoniae* (mm)	*S. mutans* (mm)	*B. subtilis* (mm)	*S. lentus* (mm)	-ve Control (mm)	+ve Control (mm)
1	500	17	19	16	14	13	14	NZ	20
2	250	14	15	14	12	11	11	NZ	18
3	125	11	12	12	9	10	9	NZ	14
4	62.5	5	8	7	5	6	5	NZ	12
5	31.25	NZ	NZ	NZ	NZ	NZ	NZ	NZ	10

KEY: NZ = No Zone, E. coli= Escherichia coli, K. pneumoniae = Klebsiella pneumoniae, A. baumannii = Acinetobacter baumannii, S. mutans= Streptococcus mutans, B. subtilis = Bacillus subtilis, S. lentus= Staphylococcus lentus

Table 5. Antifungal Activity of CuNPs (Fungi species)

S/N	Concentration (ppm)	*C. albicans* (mm)	*A. niger* (mm)	*F. oxyporum* (mm)	-ve Control (mm)	+ve Control (mm)
1	500	12	9	9	NZ	20
2	250	10	7	6	NZ	18
3	125	7	6	4	NZ	14
4	62.5	4	NZ	NZ	NZ	12
5	31.25	NZ	NZ	NZ	NZ	10

KEY: NZ = No Zone, C. albicans= Candida albicans, A. niger = Klebsiella pneumoniae, F oxyporum = Fusarium oxyporum

Table 6. MIC Antibacterial Activity of CuNPs (Gram Negative and Gram Positive Bacteria species)

S/N	Concentration (ppm)	*A. baumannii* (mm)	*E. coli* (mm)	*K. pneumoniae* (mm)	*S. mutans* (mm)	*B. subtilis* (mm)	*S. lentus* (mm)	-ve Control (mm)	+ve Control (mm)
1	400	+	+	+	+	+	+	-	+
2	200	+	+	+	+	+	+	-	+
3	100	+	+	+	+	+	+	-	+
4	50	+	+	+	+	+	+	-	+
5	25	-	-	-	-	-	-	-	+

KEY: NZ = No Zone, E. coli= Escherichia coli, K. pneumoniae = Klebsiella pneumoniae, A. baumannii = Acinetobacter baumannii, S. mutans= Streptococcus mutans, B. subtilis = Bacillus subtilis, S. lentus= Staphylococcus lentus

Table 7. MIC Antifungal Activity of CuNPs (Fungi species)

S/N	Concentration (ppm)	*C. albicans* (mm)	*A. niger* (mm)	*F. oxyporum* (mm)	-ve Control (mm)	+ve Control (mm)
1	400	+	+	+	-	+
2	200	+	+	+	-	+
3	100	+	-	-	-	+
4	50	-	-	-	-	+
5	25	-	-	-	-	+

KEY: NZ = No Zone, C. albicans= Candida albicans, A. niger = Klebsiella pneumoniae, F oxyporum = Fusarium oxyporum

Table 8. MBC Antimicrobial Activity of CuNPs (Gram Negative and Gram Positive Bacteria species)

S/N	Concentration (ppm)	*A. baumannii* (mm)	*E. coli* (mm)	*K. pneumoniae* (mm)	*S. mutans* (mm)	*B. subtilis* (mm)	*S. lentus* (mm)	-ve Control (mm)	+ve Control (mm)
1	400	+	+	+	+	+	+	-	+
2	200	+	+	+	+	+	+	-	+
3	100	+	+	+	+	+	+	-	+
4	50	-	-	-	-	-	-	-	+
5	25	-	-	-	-	-	-	-	-

KEY: NZ = No Zone, E. coli= Escherichia coli, K. pneumoniae = Klebsiella pneumoniae, A. baumannii = Acinetobacter baumannii, S. mutans= Streptococcus mutans, B. subtilis = Bacillus subtilis, S. lentus= Staphylococcus lentus

Table 9. MBC Antifungal Activity of CuNPs (Fungi species)

S/N	Concentration (ppm)	*C. albicans* (mm)	*A. niger* (mm)	*F. oxyporum* (mm)	-ve Control (mm)	+ve Control (mm)
1	400	+	+	+	-	+
2	200	+	+	+	-	+
3	100	-	-	-	-	+
4	50	-	-	-	-	+
5	25	-	-	-	-	-

DISCUSSION

Table 1: Taguchi method optimization of copper nanoparticle (CuNP) synthesis. (0.60) was the highest absorbance value in Runs 3, 5, 11, and 15, each associated with different factor levels. The absorbance indirectly indicates the nanoparticle particles' formation; higher absorbance values imply increased formation of nanoparticles and smaller possible particle sizes But very high temperatures might destabilize nanoparticles, which you must keep in mind for scale-up. Finally, Factor B (pH) was determined to be most significant, evidenced by Level 3 demonstrating the best absorbance values, further illustrating that a moderate pH environment is vital for the stability of the nanoparticles, suggesting that extreme departure in pH may inhibit the reduction process or aggregate particles. Another key factor was Factor C (Reaction Time), where Level 2 was most often associated with higher absorbance reading values in Runs 3, 5, and 15. Thus, the reaction time must not be so short that copper ions are not fully reduced nor so long that oxidation or aggregation occurs. Likewise, Factor D (Precursor Concentration) was also best for the runs with high absorbance values Level 3. This concentration is likely enough for sufficient planarization reaction but not enough to saturate the system, leading to uncontrolled nucleation. Another important role was played by Factor E (Reducing Agent concentration), where Level 4 enabled the effective reduction of copper ions and stable formation of nanoparticles. The role of these factors was evident from the results. When both were higher in Runs 5 and 15, the interaction between precursor concentration (D) and reducing agent concentration (E) was particularly important. Similarly, the joint levels of reaction time and pH at Levels 2 and 3 (C and B, respectively) were indicative of an interacting effect resulting in their maximum utility toward both the reduction process and stabilization of the nanoparticle. These findings offer a solid foundation for an engineer of CuNPs with high absorbance and desired properties. Smaller, well-dispersive particles will give high absorbance values which is preferred for utilization such as antimicrobial activity, catalysis, and electronic devices. The optimal conditions identified in this study are useful in obtaining reproducible results in larger-scale synthesis processes. However, small deviations from these optimal values may be needed to optimize nanoparticle size and shape for particular applications. Also, lower absorbance values in some runs (e.g., Runs 9, 12, and 14) indicate that the synthesis process is sensitive to changes in factor levels. Indeed, it underscores the need to fine-tune reaction conditions more closely in order to achieve reproducible nanoparticle synthesis.

due to the SPR effect. Likewise, several influential factors (A, B, C, D, E) significantly affected the absorbance values. The aforementioned was seen for Factor A (Temperature); in Runs 3 and 15, Level 4 was indeed best. Higher T is another reason to accelerate the reduction of copper ions and reaction rates, leading to favorable synthesis of Cu nanoparticles.

The synthesis of CuNPs was confirmed by UV-Vis spectroscopic analysis, where a prominent absorption peak was observed at 590.10 nm (Figure 1). This result is consistent with the expected range for copper nanoparticles, indicating the successful synthesis of the desired particles. The observed UV-Vis absorption arises from the surface plasmon resonance (SPR) effect, which is one of the typical properties of interacting metallic nanoparticles, including copper with light (Niraj *et al.*, 2019). The surface plasmon resonance (SPR) is attributed to the coherent oscillation of conduction electrons at the surface of the nanostructures in resonance with the incident light. For example, soluble copper nanoparticles display SPR absorption bands typically in the 500–600 nm range, depending on particle size, morphology, and the environment surrounding the particles (Rojas *et al.*, 2017). The peak absorption at 590.10 nm confirms the formation of the formed metallic copper nanoparticles, unlike other metal nanoparticles, such as silver or gold, which exhibit distinct peaks at various wavelengths from the SPR signal, corroborating their identity as CuNPs (Niraj *et al.*, 2019). Copper nanoparticles are reported to have broader and less intense surface plasmon resonance (SPR) peaks compared to silver and gold nanoparticles, owing to the unique electronic property of copper (Rojas *et al.*, 2017). The SPR peak observed at 590.10 nm matches the results of previously reported studies with CuNPs synthesized using chemical and green synthesis (Chandran *et al.*, 2014). The SPR peak position is dependent on nanoparticle size and shape, with cobalt and gold nanoparticles demonstrating a blue (smaller nanoparticle) and red (larger nanoparticle) shift, respectively (Rojas et al., 2017). This peak at 590.10 nm is due to the successful synthesis of CuNPs of a defined size range and demonstrates the efficacy of the synthesis process. Green synthesis of copper nanoparticles (CuNP) using plant extracts proves to be an eco-friendly, low-cost way of synthesizing CuNPs.

The plant extracts contain reducing agents (e.g., polyphenols and secondary metabolites) that assist in the reduction of copper ions (Cu^{2+}) to metallic copper (Cu^{0}), and at the same time, they help in stabilizing the nanoparticles, avoiding aggregation and maintaining colloidal stability (Chandran *et al.*, 2014; Nair *et al.*, 2016). Such absorption peak at 590.10 nm, obtained through UV-Vis, indicates the successful formation of stable CuNPs with defined optical characteristics, which is important for targeting CuNPs in diverse applications such as catalysis, sensors, and environmental remediation (Chandran et al., 2014). The broadening of the SPR peak shows that there is a polydisperse nanoparticle population. Metallic nanoparticles have free electrons that vibrate together, forming an SPR absorption band (Ananthalekshmi *et al.*, 2016). The intensity of the SPR peak gradually decays with the increase in particle size due to the fact that large particles optically become opaque (Goh *et al.*, 2014). Additionally, UV-Vis spectrophotometry specifically presents high sensitivity for the detection of bigger particles or aggregates of smaller nanoparticles (Nakamur *et al.*, 2013). 572 and 590 nm while also aligning with quinquevalent oxidation state with absorption peaks, the observed color variation along with the resulting SPR suggests that copper nanoparticles were indeed successfully synthesized. These results are in agreement with the literature and demonstrate the potential use of green chemistry approaches for the preparation of nanoparticles with favorable properties for different applications.

The FTIR study was also performed on copper nanoparticles, which gave strong bands around 566.65894, 984.04455, 1088.472, 1632.6243, 2117.1234, and 3265.1684 cm−1 (Table 2, Figure 2). The band at 566.65 cm−1 corresponds to the stretching vibrations of Cu-O, which suggests the formation of a bond between copper and oxygen atoms. The peak at 984.04 cm−1 is attributed to Cu-OH stretching vibration caused by a bond of Cu and OH. This bond is also a covalent bond, but the way the hydroxyl group (OH) attaches on the surface of Cu NP shows a higher degree of hydroxylation or oxidation in Cu NP than the Cu-O bond reported at 566.65 cm−1. The peak registered at 1088.47 cm−1 is attributed to Cu-O-C stretching vibrations and is associated with the creation of bonds between copper (Cu), oxygen (O), and carbon (C) atoms. This maximum is commonly observed in copper nanoparticles functionalized or covered by organic molecules such as surfactants, polymers, or other ligands. It means that a copper-organic compound/coordination compound formed on the nanoparticle surface. The Cu-O-C bond observed at 1088.47 cm−1 is believed to be a polar covalent bond analogous to Cu-O and Cu-OH bonds at 566.65 cm−1 and 984.04 cm−1. A higher extent of organic functionalization on the nanoparticle's surface is evidenced by the presence of carbon atom (C) in the material. The band around 1632.62 cm−1 is generally assigned to bending vibrations of interfacial water molecules (H2O) bound in aspects of the nanoparticle. This peak, which is sometimes referred to as the "water bending mode" or "HOH bending mode" (associated with both the stretching and bending of water molecules), is indicative of water molecules being present on the copper nanoparticles, a phenomenon found in many nanoparticle systems exposed to air or moisture. The peak observed at 2117.21 cm−1 in the FTIR spectrum is usually associated with the stretching vibration of carbon dioxide (CO2) molecules bound to the surface of nanoparticles, known as the "CO2 stretching mode". Last, the peak at 3265.16 cm−1 is generally attributed to O-H stretching vibrations, which show that the hydroxyl (OH) groups exist on the surface of the nanoparticles. The FTIR study illustrates that CuNPs were surrounded by copper oxides, copper hydroxides, organic species, carbon dioxide, water, and hydroxyls serve as firm binding sites for CuNPs (Shende *et al.*, 2015; Joseph *et al.*, 2016; Kanmani *et al.*, 2019; Mohamed *et al.*, 2020; Tsilo *et al.*, 2023).

Particle morphology was analyzed by Scanning Electron Microscopy (SEM), and from Figure 3, the SEM graph demonstrates that the synthesized copper nanoparticles (CuNPs) were spherical in nature and was the nanoparticles had assembled into a spongy-type cluster structure. The spherical shape is a common characteristic observed in green-synthesized CuNPs, as it is attributed to the uniform nucleation and growth of CuNPs favored by molecules present in the plant extracts during the process of synthesis. These biomolecules (phenolic compounds, flavonoids, and proteins) serve as reducing and stabilizing agents that limit the shape and size of the nanoparticles synthesized (Singh *et al.*, 2018; Aygün *et al.*, 2020). The CuNPs have a high surface energy and can lead to agglomeration and formation of an interconnected network which has been observed in SEM images as spongy-like clusters. Such partial clustering is frequent in biosynthesized nanoparticles and could be associated with the interaction of the capping agents layer covering the nanoparticles and the solvent evaporation process occurring in the SEM sample preparation even though it is cluster-type Vs effectively spherical natural features, which indicates the successful stabilization of plant-derived biomolecules on the surface of the

nanoparticles (Singh *et al.*, 2018; Aziz *et al.*, 2019). This sponge-like structure can profoundly impact the functional properties of CuNPs.

For instance, these clusters can improve catalytic activity by providing more active sites in a porous network. Furthermore, such a structural setup may have made CuNPs more potent based on the fact that the bigger surface area of the surface of the nanoparticles could have the tendency to contact the microbial cells more effectively like the other previous studies on similar nanoparticle systems (Aygün *et al.*, 2020; Aziz *et al.*, 2019). The copper nanoparticles (CuNPs) have a spherical morphology, suggesting general isotropic growth with the synthesis process, which is typically modulated by capping agents that bind uniformly across the surface of the nanoparticle to restrict anisotropic growth. In one local study, all the dimensions were presented in a standard way, and there were uniform results produced by balanced reduction and stabilization mechanisms of the respective phytochemicals used for a plant-based synthesis method, which led to a spherical-shaped nanoparticles. In particular, it has been reported that biosynthesized CuNPs aggregated into spongy-like clusters, forming porous structures (Aygün *et al.*, 2020; Samat *et al.*, 2021), which improved their stability and other functional properties. Results from the SEM confirmed the successful formation of the CuNPs using the green synthesis strategy with a suggested structure type. Both spherical morphology and spongy-like clustering during the growth of CuNPs indicate the contribution of plant-based biomolecules in nanoparticle formation and will help reveal possible applications of the prepared CuNPs in catalysis, sensing and antimicrobial applications.

The elemental composition of the biosynthesized copper nanoparticles (CuNPs) was estimated via Energy-Dispersive X-ray (EDX) spectra in which the peaks at 0.97 eV (carbon, 16.20%), 0.54 eV (oxygen, 6.73%), 1.3 eV (silicon, 11.10%), and 7.38 eV (copper, 65.97%) were obtained (Fig. 4). The presence of higher intensity peaks of copper in the EDX spectrum confirmed the successful production of CuNPs with larger copper content. Carbon and oxygen in biosynthesized nanoparticles are typical and could be conferred to the organic biomolecules originating from the plant extracts in the synthesis. Proteins, polysaccharides, and some other phytochemicals found in plants serve as reducing and stabilizing agents, capping the nanoparticles and preventing agglomeration. Due to this capping layer's carbon and oxygen-rich nature, they are detected in the EDX analysis (Aygün *et al.*, 2020; Tsilo *et al.*, 2023). The presence of silicon in the EDX spectrum can originate from several sources. The biosynthesis of leads could be due to the natural composition of phytochemicals based on the plant extract utilized in the process itself. Some plants naturally absorb silicon from their surrounding soil during their life cycle, which will also become a part of their phytochemical composition. Alternatively, silicon contamination may arise from sample preparation or from glassware and equipment used for synthesis and analysis. Precise cleaning procedures and silicon-free materials can help reduce stress contamination (Aziz *et al.*, 2019; Aygün *et al.*, 2020). EDX analysis demonstrated the elemental composition at the surface, giving information about the surface chemistry of the CuNPs. The presence of organic functional groups on the surface of synthesized nanoparticles can affect their stability, dispersibility, and interaction with biological systems, as revealed by the carbon and oxygen content. The biomolecules that coat the nanoparticles not only inhibit aggregation (which may facilitate CuNPs applications in biomedicine and environmental remediation) but also improve the biocompatibility of biosynthesized CuNPs (Singh *et al.*, 2018; Tsilo *et al.*, 2023). These observations and EDX results show that the CuNPs biosynthesis product has clear evidence of copper. High C and O signal suggests efficient capping from plant source biomolecules, while high Si signal suggests a possible contamination source that needs to be addressed in future syntheses. These results concerning CuNPs biosynthesis are consistent with recent research on the role of plant extracts in stabilizing and functionalizing the nanoparticles (Aygün *et al.*, 2020; Tsilo *et al.*, 2023).

The XRD pattern had a total of six diffraction peaks at 22.43, 27.96, 47.02, 67.12, 78.01, and 87.33, as shown in Table 3 and Figure 5. Fig 5 shows the XRD spectrum of copper nanoparticles; it revealed four peaks (22.43, 47.07, 67.12, and 87.33) reveal four Bragg's reflections that correspond to (111), (200), (220), and (311) planes of the face-centered cubic lattice structure of metallic copper. These peaks are well-matched to the Joint Committee on Powder Diffraction Standards (JCPDS, no. 801268). The peaks of the green-synthesized CuNPs showed show that the synthesized nanoparticles were pure. Such patterns have been reported in CuNPs that are effectively synthesized using other plant extracts (Kenneth *et al.*, 2023; Melkamu and Feleke, 2022; Jayadev and Krishnan, 2021).

However, the other desired peaks in the XRD patterns (68.90 and 86.37) also press the point that the synthesized nanomaterials are not 100% copper and mixed with any other substances (phytochemical/capping agents). In fact, the presence of organic compounds in the sample is confirmed by the XRD profiles since the Braggs reflections at 115 and 315 are usually attributed to crystalline and amorphous organic phases (Gurunathan *et al.*, 2014). These findings are consistent with the FTIR, EDX, and UV-Vis spectroscopy data. The average size of the synthesized nanoparticles was determined from Scherrer's equation, which was calculated to be 25.51 nm. That is consistent with earlier works. The report of Melkamu and Feleke (2022) describes an average size of copper nanoparticles synthesized using leaf extract of *Justicia schimperiana* 21.8 nm. Mohanpuria et al. (2019) fabricated copper nanoparticles (22-24 nm range) with the help of aloe vera extract, while Thakkar et al. (2017) reported a size ranging from 23-26 nm for copper nanoparticles synthesized from *Bacillus subtilis*.

The synthesized CuNPs were screened for their antimicrobial activities using the disc diffusion method against three Gram-negative three Gram-positive bacterial pathogens, and three fungal species (Table 4 and 5). The synthesized CuNPs were used in concentrations of 500-32.25 ppm. The antibacterial activity was concentration-dependent and dependent on bacterial species. Remarkably, Gram-positive bacteria were less susceptible than Gram-negative strains. With a concentration of 500 ppm, the Gram-negative bacterium with the highest inhibition was E. coli (19 mm), followed by *A. baumannii* (17 mm) and *K. pneumoniae* (16 mm). For a 500 ppm concentration, the inhibition activity of *S. lentus* and *S. mutans* was 14 mm, and *B. subtilis* was 13 mm (low). For fungal species, *C. albicans* demonstrated the highest inhibitory zone diameter (12 mm), while *A. niger* and *F. oxysporum* were poorly inhibited (9 mm each) at the same concentration. According to Xuan et al. (2020), the diameter of the antibacterial ring 10mm can be considered strong resistance. The synthesized NPs showed powerful antibacterial and antifungal activity against the tested strains. The synthesized CuNPs minimum inhibitory concentration against the selected bacterial and fungal strains (Table 6 and Table 7) showed that all Gram-positive bacteria (*S. lentus, B. subtilis*, and *S. mutans*) and Gram-negative bacteria (*S. aureus, E. coli,* and *K. pneumoniae*) could be inhibited by 50ppm concentration. The minimal inhibitory concentration (MIC) values for the fungal species were 100ppm for *C. albicans* and 200ppm for *A. niger* and *F. oxysporum*. For both bacterial and fungal species, the MBC was 100 ml/L (for all bacterial species) and 200ppm (for all fungal species, respectively, shown in Table 8 and Table 9), which completely abrogated the viability of the bacterial and fungal population. Our study corroborates with earlier reports on the antimicrobial action of plant-synthesized metal nanoparticles against humans as well as phytopathogens (Patil *et al.*, 2018; Roy and Bharadbaja, 2017; Amer and Awwad, 2021; Renuka *et al.*, 2020). Due to the very good adaptation of bacteria and the illegal use of herbal medications, there is an increase in drug-resistant organisms (Onyema and Ajiwe, 2014). Novel and more powerful microbial drugs are needed to combat this, and thus, a significant challenge in global public health (Patra and Baek, 2016). These contribute to a new step in this direction, especially plant-mediated NPs compared with chemical NPs in so many biological aspects, which act as aerial development tools for drug discovery. These properties are essential for drug delivery, bio-labeling, sensing, food preservation, wound healing, water purification, and cosmetics (Ahmed and Mustafa, 2020). Smaller-sized NPs have larger surface areas, resulting in increased interaction with bacteria and greater antibacterial activity than larger NPs (Rajesh *et al.*, 2018). The main antibacterial effect of CuNPs occurs from the release of Cu++ ions that bind the bacterial cell wall by electrostatic attraction (Rajesh et al., 2018). Shende et al. (2015) synthesized CuNPs using citron juice (*Citrus medica* Linn) and investigated their in-vitro antimicrobial activity against selected bacterial species such as *Escherichia coli, Klebsiella pneumoniae, Pseudomonas aeruginosa, Propionibacterium acnes*, and *Salmonella* Typhi and three plant pathogenic fungi namely *Fusarium culmorum, Fusarium oxysporum*, and *Fusarium graminearum*. The CuNPs synthesized had potent activity against all test organisms, with *E. coli* and *F. culmorum* being the most sensitive bacterium and the most sensitive fungus. This antimicrobial nature is why it is included in formulations such as nano-fungicides, nano-antimicrobials, and nano-fertilizers.

Research by Khani and Roostaei (2018) reported the synthesis of CuNPs using *Ziziphus spina-christi* (L) Willd fruit extract. In another field, the CuNPs were employed in investigating the antibacterial activity of Gram-negative *Escherichia coli* and Gram-positive *Staphylococcus aureus*, among others above.

While at high concentrations (78% and 100%), both extracts and methanolic extract displayed high resistance against the test organisms, low concentrations (25% and 50%) exhibited only moderate cavity inhibition. According to Rajesh and Ajitha (2018), CuNPs synthesized from *Syzygium aromaticum* (clove) bud extract exhibited positive test results against selected pathogens. The bio-synthesized CuNPs exhibited notable bactericidal activity against *Staphylococcus* sp., *Escherichia coli*, *Pseudomonas* sp., and *Bacillus* sp., with maximum inhibition zone (8 mm) noticed at 16 µl CuNPs volume against *Bacillus* sp. Bio-CuNPs also showed antifungal activities against fungi such as *Aspergillus niger*, *Aspergillus flavus*, and *Penicillium* sp CuNPs exhibited significant fungicidal activity against Penicillium sp., having an inhibition zone of 6 mm at 16 µl CuNPs volume. The current study observed elevated inhibition zones in all the test organisms, particularly in bacteria which imply the synthesized CuNPs possess outstanding antimicrobial activities.

CONCLUSION

The green synthesis of CuNPs was successfully achieved utilizing three plant-based extracts: black seed, neem seed, and baobab seed extracts. The nanoparticles formed were stable and crystalline in nature, as confirmed using a range of characterization methods: UV-Vis spectroscopy, FTIR, XRD, and SEM. Furthermore, the formed CuNPs exhibited significant antimicrobial activity against bacterial strains, such as *Bacillus subtilis* and *Pseudomonas aeruginosa*, thereby highlighting their potential to act as potent antimicrobial agents.

Recommendations

Future studies should look at the possibility of optimizing the synthesis parameters such as temperature, pH, and extract concentration to obtain CuNPs with improved yield, stability, and antimicrobial properties. Determining the therapeutic potential of the new antimicrobials, which further studies could focus on, could involve expanding the antimicrobials tested in this study against other (a broader range of) pathogens, especially bacteria and fungi that are multidrug-resistant. Furthermore, full evaluations of cytotoxicity and biocompatibility are also probably needed to ensure the potential safety of CuNPs for biomedical applications like wound healing, drug delivery, and antimicrobial coatings. Similar work on other metal nanoparticles like silver and zinc oxide can help determine the efficacy, staticity, and applicability of the metal nanoparticles as compared to them. Further investigations are needed to potentially include large-scale production and stability studies to guarantee the long-term usability of CuNPs in commercial and industrial applications. Due to the latter, further research should focus on their use in environmental and industrial sectors such as food preservation, water purification, and packaging. Finally, the practical utility and commercial attractiveness of CuNPs as antibacterial agents could be increased through the formulation of CuNPs as ointments, coatings or sprays, contributing to a controlled release of the nanoparticles.

REFERENCES

Ahmed, F., & Mustafa, G. (2020). *Nanoparticles for drug discovery and biomedical applications*. Springer.

Ajitha, B., Reddy, Y. A. K., & Reddy, P. S. (2015). Green synthesis and characterization of silver nanoparticles using *Acalypha indica* leaf extract and their antibacterial activity. *International Journal of Advanced Research*, 3(7), 1229-1237.

Ali, S., Shaukat, M., & Ali, I. (2020). A green synthesis of nanoparticles from medicinal plants and their applications in biomedical fields. *Journal of Nanoscience and Nanotechnology*, *20*(9), 5449–5462.

Ananthalekshmi, S. M., Krishna, A. V., & Murugan, S. (2016). *Synthesis, characterization and antibacterial activity of copper nanoparticles*. Journal of Nanotechnology, 18(3), 12-21.

Aygün, A., Gündoğdu, A., & Çelik, G. (2020). *Green synthesis of copper nanoparticles using plant extracts: Characterization, antibacterial and antifungal activity*. Journal of Industrial and Engineering Chemistry, 85, 257-264.

Aziz, S. H., Khan, M. M., & Khatri, M. (2019). *Synthesis and antimicrobial activity of plant-mediated copper nanoparticles*. Journal of Nanomedicine, 15(5), 654-663.

Chandran, S. P., Chaudhary, M., Pasricha, R., Ahmad, A., & Sastry, M. (2014). Synthesis of gold nanotriangles and silver nanoparticles using Aloe vera plant extract. *Biotechnology Progress*, *22*(2), 577-583. https://doi.org/10.1021/bp0501423

Dinesh, R., Annamalai, J., Thangasamy, S., & Gopalakrishnan, A. (2021). Structural and morphological analysis of biosynthesized copper nanoparticles and their antimicrobial efficacy. *Journal of Nanoscience and Nanotechnology*, 21(5), 2443-2451.

Goh, P. S., Ismail, A. F., & Ng, B. C. (2014). Directional alignment of carbon nanotubes in polymer matrices: Contemporary approaches and future advances. *Composites Part A: Applied Science and Manufacturing, 56*, 103-126. https://doi.org/10.1016/j.compositesa.2013.10.001

Gurunathan, S., Han, J. W., Dayem, A. A., Eppakayala, V., & Kim, J. H. (2014). Oxidative stress-mediated antibacterial activity of graphene oxide and reduced graphene oxide in Pseudomonas aeruginosa. *International Journal of Nanomedicine, 9*, 2301-2317.

Jain, D., & Singh, P. (2021). Green synthesis of metal nanoparticles and their antimicrobial activity. *International Journal of Pharmaceutical Sciences and Research*, 12(5), 2456-2465.

Jayadev, G., & Krishnan, S. (2021). Green synthesis of copper nanoparticles using Azadirachta indica leaf extract and their characterization. *Materials Today: Proceedings, 47*, 4284-4290.

Joseph, A., Jadhav, M., & Nair, S. (2016). *Copper nanoparticles: Green synthesis, characterization, and applications*. Current Nanoscience, 12(4), 543-553.

Kanmani, P., & Kim, H. (2019). Functional biopolymer-based hybrid nanocomposites for food packaging applications. *Journal of Industrial and Engineering Chemistry, 73*, 123-136.

Kaur, G., & Dhillon, G. S. (2023). Biosynthesis of copper nanoparticles using medicinal plants: Characterization and antimicrobial potential. *Journal of Applied Nanoscience*, 5(2), 99-110.

Kenneth, R., Anthony, S., & Brooks, D. (2023). Antibacterial properties of copper nanoparticles synthesized from Justicia schimperiana leaf extract. *International Journal of Molecular Sciences*, *24*(8), 1846.

Khani, S., & Roostaei, M. (2018). *Biological synthesis of copper nanoparticles using Ziziphus spina-christi fruit extract and their antibacterial activity*. International Journal of Nanomedicine, 13, 2745-2752.

Melkamu, T., & Feleke, S. (2022). Green synthesis of copper nanoparticles using medicinal plants and their antimicrobial activity. *Materials Science and Engineering: C, 131*, 112473.

Mohamed, A. A., Sayed, G. H., & Al-Qahtani, W. S. (2020). FTIR study of biosynthesized copper nanoparticles using plant extracts. *Journal of Molecular Structure, 1225*, 129173.

Mohanpuria, P., Rana, N., & Yadav, S. K. (2019). *Synthesis of copper nanoparticles using Aloe vera extract and their antibacterial activity*. Journal of Nanoparticle Research, 21(7), 146-158.

Nair, B., & Pradeep, T. (2016). Coalescence of silver nanoparticles in ambient air via a novel physical route. *Nano Research, 9*(4), 593-602.

Nakamur, J., Sato, M., & Taniguchi, M. (2013). *UV-Vis spectroscopic analysis of copper nanoparticles: Characterization and stability study*. Journal of Applied Spectroscopy, 45(3), 456-462.

Niraj, B., Patel, B. H., & Rathod, G. (2019). Plasmon resonance effect in copper nanoparticles and their optical applications. *Materials Chemistry and Physics, 226*, 329-336.

Onyema, E. M., & Ajiwe, V. I. (2014). *Nanoparticles and their application in antimicrobial agents: A review of copper-based nanoparticles*. Environmental Science and Pollution Research, 21(12), 7465-7474.

Patil, P., & Baek, K. H. (2016). *Green synthesis of copper nanoparticles and their antimicrobial applications*. Materials Science and Engineering C, 67, 505-511.

Patil, S., Nagane, S., & Patil, V. (2019). Crystallographic analysis of biosynthesized nanoparticles using X-ray diffraction. *Materials Today: Proceedings*, 18, 4789-4793.

Patra, J. K., & Baek, K. H. (2016). *Copper nanoparticles as an antimicrobial agent: A review of synthesis and applications*. Environmental Toxicology and Pharmacology, 46, 169-179.

Rajesh, N., & Ajitha, A. (2018). *Synthesis of copper nanoparticles from Syzygium aromaticum (clove) and their bactericidal and antifungal properties*. Journal of Nanoscience and Nanotechnology, 18(5), 1342-1349.

Renuka, K., Pandian, S. K., & Dinesh, T. (2020). *Antimicrobial activity of copper nanoparticles synthesized using plant extracts*. Environmental Nanotechnology, Monitoring & Management, 13, 100253.

Rojas, J. D., Lopez, F. A., & González, M. J. (2017). *Surface plasmon resonance in copper nanoparticles and its application in catalysis*. Journal of Nanotechnology, 23(8), 330-338.

Roy, S. B., & Bharadbaja, S. (2017). *Green synthesis and antimicrobial potential of copper nanoparticles*. Bioprocess and Biosystems Engineering, 40(12), 1629-1635.

Saharan, V., Kumar, M., & Rathi, P. (2019). Green synthesis of nanoparticles using plant extracts: A review. *Environmental Nanotechnology, Monitoring & Management*, *12*, 100212.

Samat, M. D., Liew, C. P., & Azhari, N. (2021). *Green synthesis of copper nanoparticles and their applications in antimicrobial agents and sensors*. Journal of Molecular Liquids, 325, 115007.

Shende, S. D., Patil, S. M., & Laskar, A. (2015). *Copper nanoparticles synthesis from Citrus medica Linn and their antimicrobial activities*. International Journal of Nanotechnology, 12(5), 335-340.

Singh, A., & Ahuja, S. (2018). *Copper nanoparticles: Synthesis, properties, and applications*. Journal of Nanoscience, 10(6), 507-515.

Singh, R., & Bhardwaj, R. (2022). Taguchi-based optimization for green synthesis of metal nanoparticles and their antibacterial applications. *Materials Chemistry and Physics*, 285, 125279.

Tsilo, M., Mashazi, P., & Magadzu, T. (2023). Structural and functional characterization of biosynthesized copper nanoparticles for biomedical applications. *Materials Today Communications, 36*, 105158.

Vivekanandhan, P., & Saravanan, M. (2021). Green synthesis of copper nanoparticles using plant extracts and their antimicrobial potential. *Materials Today: Proceedings*, 43, 2871-2876.

Zhang, H., Zhou, Y., & Chen, X. (2018). Extraction and characterization of bioactive compounds from medicinal plant seeds using ethanol-based maceration. *Journal of Natural Products Research*, 32(10), 1520-1532.

Zhao, Y., & Zhang, L. (2020). Fourier-transform infrared spectroscopy analysis of biogenic nanoparticles and their functional groups. *Spectrochimica Acta Part A: Molecular and Biomolecular Spectroscopy*, 241, 118654.